Linear stability of a doubly periodic array of vortices to three-dimensional perturbations

A. K. Pathak and S. N. Bhattacharyya

Citation: Physics of Fluids **22**, 054105 (2010); doi: 10.1063/1.3415135
View online: http://dx.doi.org/10.1063/1.3415135
View Table of Contents: http://scitation.aip.org/content/aip/journal/pof2/22/5?ver=pdfcov
Published by the AIP Publishing

Linear stability of a doubly periodic array of vortices to three-dimensional perturbations

A. K. Pathak and S. N. Bhattacharyya
Department of Mechanical Engineering, Indian Institute of Technology, Kharagpur 721302, West Bengal, India

(Received 5 December 2008; accepted 16 March 2010; published online 11 May 2010)

The linear stability of a doubly periodic array of vortices to three-dimensional perturbations is studied. The instabilities are separated into symmetric and antisymmetric modes. For two-dimensional disturbances only the symmetric mode is found to be unstable. The antisymmetric mode shows a peak in growth rate at long wavelengths. This is attributed to the Crow instability. For short wavelengths both symmetric and antisymmetric modes are found to have similar growth rates. This is attributed to the elliptical instability and it is found to occur even when the vortex cells are square, a physical explanation for which is provided, but for elongated vortex cells the growth rates are higher. Viscosity is found to have a strong stabilizing influence on short wavelength perturbations. © *2010 American Institute of Physics*. [doi:10.1063/1.3415135]

I. INTRODUCTION

Interest in arrays of vortices arose from observation of the vortex pattern in the wake of an object placed in a flowing stream of fluid. A staggered double row of contrarotating vortices, with a street spacing ratio (the ratio of distance between the two rows to the separation of the vortices in the same row) of $\cosh^{-1}(\sqrt{2})/\pi \approx 0.281$ is observed. A linear stability study for two-dimensional perturbations shows that it is only for this value of the street spacing that the configuration is stable. This stability analysis is discussed in textbooks on hydrodynamics.[1,2] It considers the vortices to be point vortices in the two-dimensional model. The difficulty with point vortices is that, apart from giving rise to infinite velocity at the vortex center, which is physically unrealistic, this also leads to divergences when stability to three-dimensional disturbances is considered, and these have to be removed by assuming some cutoff. Therefore, it would be more realistic to consider a configuration where the vortices have a finite area of cross section. One such solution of the equations governing two-dimensional flow of an incompressible, inviscid fluid was found by Stuart.[3] This gives a row of identical vortices. Mallier and Maslowe[4] obtained another solution which gives a row of counter-rotating vortices. More recently solutions which give doubly periodic arrays of vortices have been obtained.[5–10]

Stability studies of some of these configurations of vortex arrays have been carried out. Pierrehumbert and Widnall[11] studied the stability of Stuart vortices[3] to two- and three-dimensional perturbations. They identified the instabilities that would occur and showed that their theoretical predictions were in good agreement with experimental observations. Dauxois[12] and Dauxois *et al.*[13] studied the stability of the Mallier and Maslowe vortices[4] to two-dimensional perturbations. Subsequently, Julien *et al.*[14] carried out a three-dimensional stability analysis for this configuration and showed that the fastest growing modes are three-dimensional in nature. They explained their results in terms of the Crow instability,[15] a long wavelength instability of a pair of counter-rotating line vortices, and the elliptical instability,[16–18] which occurs at shorter wavelengths in noncircular vortices. While the importance of carrying out stability studies for the configurations reported in Refs. 5–10 is recognized, so far only a stability study restricted to two-dimensional perturbations has been reported.[9] However, the stability of another configuration of a doubly periodic array of vortices, known as the flattened Taylor–Green vortices, for three-dimensional disturbances has been reported.[19] We carry out a similar study for one of the doubly periodic vortex array solutions reported in Ref. 8 and compare our results with those in Ref. 19.

While the initial interest in vortex arrays arose in the context of vortex shedding and the formation of a Kármán street, renewed interest in some of these vortex array configurations has come for a different reason. Some of these configurations of vortex arrays satisfy the sinh-Poisson equation

$$\frac{\partial^2 \psi}{\partial x^2} + \frac{\partial^2 \psi}{\partial y^2} = -\sigma \sinh \psi,$$

where ψ is the stream function and σ is a constant, and it has been shown that one solution for the most probable states for two-dimensional, incompressible, inviscid flow are governed by the sinh-Poisson equation.[20] Further it was demonstrated[21,22] by numerical simulations that even when viscosity is present the flow relaxes toward the maximum entropy state governed by the sinh-Poisson equation. Motivated by these theoretical considerations, experiments have been carried out to study linear[23] and two-dimensional arrays[24,25] of vortices, similar to solutions of the sinh-Poisson equation.

In this article we carry out a linear stability analysis for a doubly periodic vortex array solution described in Ref. 8. In Sec. II, we define the physical problem and describe our method for carrying out the stability analysis. In Sec. III, we

provide results of the stability study for a doubly periodic vortex array. In Sec. IV, we discuss our findings and identify directions for further work.

II. FORMULATION

The governing equations for a viscous incompressible flow are

$$\frac{\partial \mathbf{v}}{\partial t} + \mathbf{v} \cdot \nabla \mathbf{v} = -\nabla\left(\frac{p}{\rho}\right) + \nu \nabla^2 \mathbf{v} + \mathbf{f}, \tag{1}$$

$$\nabla \cdot \mathbf{v} = 0, \tag{2}$$

where ρ, ν, p, and $\mathbf{v}$ are the density, kinematic viscosity, pressure, and velocity of the fluid and $\mathbf{f}$ is the acceleration field due to an external force which maintains the array of vortices even in the presence of viscosity. Alternatively, in the absence of the acceleration field $\mathbf{f}$, we have a decaying vortex solution. We can still assume a steady unperturbed state provided the perturbations evolve on a sufficiently faster time scale so that on that time scale the decay of the unperturbed vortices can be neglected. In writing Eq. (1), it has been assumed that ρ is constant. We assume an unperturbed configuration described in a Cartesian coordinate system (x,y,z) by

$$\mathbf{v} = U(x,y)\mathbf{e}_x + V(x,y)\mathbf{e}_y, \quad \frac{p}{\rho} = P(x,y), \tag{3}$$

which represents a two-dimensional flow. We consider a small perturbation from this configuration given by

$$\mathbf{v} = (U+u)\mathbf{e}_x + (V+v)\mathbf{e}_y + w\mathbf{e}_z, \quad \frac{p}{\rho} = P + \varpi, \tag{4}$$

where the perturbations u, v, w, and ϖ are functions of x, y, z, and t. Substituting in Eqs. (1) and (2), linearizing in the perturbations, and assuming normal modes with (t,z)-dependence of the form $\exp(\sigma t + i\alpha z)$, we obtain

$$\sigma u = \mathcal{L}_{11}u + \mathcal{L}_{12}v + \mathcal{L}_{14}\varpi, \tag{5}$$

$$\sigma v = \mathcal{L}_{21}u + \mathcal{L}_{22}v + \mathcal{L}_{24}\varpi, \tag{6}$$

$$\sigma w = \mathcal{L}_{33}w - i\alpha\varpi, \tag{7}$$

$$\mathcal{L}_{41}u + \mathcal{L}_{42}v + i\alpha w = 0, \tag{8}$$

where

$$\mathcal{L}_{11} = \mathcal{L}_{33} - \frac{\partial U}{\partial x}, \quad \mathcal{L}_{12} = -\frac{\partial U}{\partial y}, \quad \mathcal{L}_{14} = -\frac{\partial}{\partial x},$$

$$\mathcal{L}_{21} = -\frac{\partial V}{\partial x}, \quad \mathcal{L}_{22} = \mathcal{L}_{33} - \frac{\partial V}{\partial y}, \quad \mathcal{L}_{24} = -\frac{\partial}{\partial y},$$

$$\mathcal{L}_{33} = -U\frac{\partial}{\partial x} - V\frac{\partial}{\partial y} + \nu\left(\frac{\partial^2}{\partial x^2} + \frac{\partial^2}{\partial y^2} - \alpha^2\right),$$

$$\mathcal{L}_{41} = \frac{\partial}{\partial x}, \quad \mathcal{L}_{42} = \frac{\partial}{\partial y}.$$

Eliminating w between Eqs. (7) and (8), we obtain

$$\alpha^2\varpi = -\sigma(\mathcal{L}_{41}u + \mathcal{L}_{42}v) + \mathcal{L}_{33}(\mathcal{L}_{41}u + \mathcal{L}_{42}v). \tag{9}$$

Substituting in Eqs. (5) and (6) we readily obtain

$$\mathcal{A}\begin{Bmatrix} u \\ v \end{Bmatrix} = \sigma\mathcal{B}\begin{Bmatrix} u \\ v \end{Bmatrix}, \tag{10}$$

where

$$\mathcal{A} = \begin{bmatrix} \alpha^2\mathcal{L}_{11} + \mathcal{L}_{14}\mathcal{L}_{33}\mathcal{L}_{41} & \alpha^2\mathcal{L}_{12} + \mathcal{L}_{14}\mathcal{L}_{33}\mathcal{L}_{42} \\ \alpha^2\mathcal{L}_{21} + \mathcal{L}_{24}\mathcal{L}_{33}\mathcal{L}_{41} & \alpha^2\mathcal{L}_{22} + \mathcal{L}_{24}\mathcal{L}_{33}\mathcal{L}_{42} \end{bmatrix}, \tag{11}$$

$$\mathcal{B} = \begin{bmatrix} \alpha^2\mathcal{I} + \mathcal{L}_{14}\mathcal{L}_{41} & \mathcal{L}_{14}\mathcal{L}_{42} \\ \mathcal{L}_{24}\mathcal{L}_{41} & \alpha^2\mathcal{I} + \mathcal{L}_{24}\mathcal{L}_{42} \end{bmatrix}, \tag{12}$$

and $\mathcal{I}$ is the identity operator. Equation (10) is the eigenvalue problem for the growth rate σ. The existence of an eigenvalue σ with positive real part implies instability.

In order to solve Eq. (10), for the doubly periodic vortex array, we assume for u and v the representations

$$u = \sum_{n=-N}^{N}\sum_{m=-M}^{M} u_{mn} e^{im\pi x/L} e^{in\pi y/L_1},$$

$$v = \sum_{n=-N}^{N}\sum_{m=-M}^{M} v_{mn} e^{im\pi x/L} e^{in\pi y/L_1}, \tag{13}$$

where u_{mn} and v_{mn} are constants. The representations would be exact if $M,N\to\infty$, but for computation we have to truncate the series at finite values of M and N. In writing Eq. (13), we have assumed that the unperturbed vortex configuration is periodic in x and y with periods $2L$ and $2L_1$ and that u and v are also periodic with the same periods in x and y. A similar assumption is made in Ref. 14 for the three-dimensional stability study of a row of counter-rotating vortices. As a consequence this does not consider subharmonic modes and, therefore, does not model the pairing instability. We now consider the effect of an arbitrary linear operator $\mathcal{L}$ acting on a field variable f. Let us say

$$g = \mathcal{L}f. \tag{14}$$

Assuming that both f and g have representations similar to those in Eq. (13), it can be readily shown that

$$g_{m'n'} = \sum_{n=-N}^{N}\sum_{m=-M}^{M} L_{m'n'mn} f_{mn}, \tag{15}$$

where

$$L_{m'n'mn} = \frac{1}{4LL_1}\int_{-L_1}^{L_1}\int_{-L}^{L} e^{-im'\pi x/L} e^{-in'\pi y/L_1} \times \mathcal{L}[e^{im\pi x/L} e^{in\pi y/L_1}]dxdy. \tag{16}$$

Thus the operator $\mathcal{L}$ has been replaced by a matrix acting on the coefficients in the expansion assumed. In this way, the operators $\mathcal{A}$ and $\mathcal{B}$ in Eq. (10) can be replaced by equivalent

TABLE I. Growth rates for the linear stability of Mallier–Maslowe array of counter-rotating vortices for Re=400.

	Growth rate	
k	Antisymmetric	Symmetric
	$C=0.75$	
0.5	0.2089	0.0735
2.5	0.2933	0.3030
4.5	0.2322	0.2355
	$C=0.5$	
0.5	0.1447	0.1200
2.5	0.1462	0.1461
4.5	0.0728	0.0748

matrices. This method can also be used to study the stability of a single row of vortices, say the Mallier and Maslowe vortices,[4] by assuming the expansions

$$u=\sum_{n=0}^{N}\sum_{m=-M}^{M}u_{mn}e^{imx}e^{-y^2/2}H_n(y),$$
$$v=\sum_{n=0}^{N}\sum_{m=-M}^{M}v_{mn}e^{imx}e^{-y^2/2}H_n(y), \tag{17}$$

where $H_n(y)$ are Hermite polynomials,[26] and in this case

$$L_{m'n'mn}=\frac{1}{2\pi 2^{n'}n'!\sqrt{\pi}}\int_{-\infty}^{\infty}\int_{-\pi}^{\pi}e^{-im'x}e^{-y^2/2}H_{n'}(y)\times\mathcal{L}[e^{imx}e^{-y^2/2}H_n(y)]dxdy. \tag{18}$$

Here, it has been assumed that the unperturbed configuration is periodic along x with period 2π and that the perturbations have the same periodicity. We now use this method to compute growth rates for a row of counter-rotating vortices, described in Ref. 4, and for a doubly periodic array of vortices, described in Ref. 8. Linear stability calculations for the Mallier and Maslowe vortices have already been reported and we repeat the calculations with our method to serve as a check on our method.

For the Mallier and Maslowe[4] vortices the unperturbed flow is obtained from the stream function

$$\psi=\log\left(\frac{\cosh Cy-C\cos x}{\cosh Cy+C\cos x}\right), \tag{19}$$

where C is a constant. This produces a row of counter-rotating vortices and the pattern is periodic in x with period 2π. It can be readily shown that the magnitude of the circulation Γ around any one vortex is 4π. Julien *et al.*[14] defined the Reynolds number as $\mathrm{Re}=\Gamma/4\pi\nu$, which reduces to the simple relation $\mathrm{Re}=1/\nu$. Growth rates of the fastest growing mode for a few values of C and k for Re=400, for antisymmetric and symmetric modes, computed using our method with $M=N=10$, are given in Table I. These are seen to be in fairly good agreement with the graphs in Ref. 14.

For the doubly periodic array of vortices we consider the solution discussed in Ref. 8, where the stream function is

$$\psi=4\tanh^{-1}\left\{A_0\left[\frac{\mathrm{dn}(rx,k)}{(1-k^2)^{1/4}}-\frac{(1-k^2)^{1/4}}{\mathrm{dn}(rx,k)}\right]\times\left[\frac{\mathrm{dn}(sy,k_1)}{(1-k_1^2)^{1/4}}-\frac{(1-k_1^2)^{1/4}}{\mathrm{dn}(sy,k_1)}\right]\right\}. \tag{20}$$

Here $\mathrm{dn}(rx,k)$ and $\mathrm{dn}(sy,k_1)$ are Jacobian elliptic functions.[27–29] The amplitude function A_0 is given by

$$A_0=\frac{s(1-k_1^2)^{1/4}}{2r(1-\sqrt{1-k^2})}, \tag{21}$$

and the wavenumbers and the moduli of the elliptic functions are related by

$$s^2(1-k_1^2)^{1/4}[1-\sqrt{1-k_1^2}]=r^2(1-k^2)^{1/4}[1-\sqrt{1-k^2}]. \tag{22}$$

It is known[27] that the Jacobian elliptic function $\mathrm{dn}(u,k)$, where u is real, is periodic in u with period $2K$, where K is the complete elliptic integral of the first kind, defined by

$$K(k)=\int_0^{\pi/2}\frac{d\phi}{\sqrt{1-k^2\sin^2\phi}}.$$

Therefore, the doubly periodic vortex array, given by Eq. (20) is periodic in x and y with periods $2L$ and $2L_1$, where

$$L=\frac{K(k)}{r},\quad L_1=\frac{K(k_1)}{s}. \tag{23}$$

Here $K(k)$ and $K(k_1)$ again represent complete elliptic integrals of the first kind. The magnitude of the circulation around any one vortex or cell is given by

$$\Gamma=32A_0\left(\frac{k^2r}{1+k'}\right)\left(\frac{1}{s\sqrt{k_1'}}\right)\left[\sin^{-1}\left(\frac{1}{\sqrt{1+k_1'}}\right)-\tan^{-1}(\sqrt{k_1'})\right]+32A_0\left(\frac{k_1^2s}{1+k_1'}\right)\left(\frac{1}{r\sqrt{k'}}\right)\times\left[\sin^{-1}\left(\frac{1}{\sqrt{1+k'}}\right)-\tan^{-1}(\sqrt{k'})\right], \tag{24}$$

where $k'=\sqrt{1-k^2}$ and $k_1'=\sqrt{1-k_1^2}$. We define the Reynolds number as $\mathrm{Re}=\Gamma/\nu$.

The unperturbed configuration for the doubly periodic vortex array has symmetry similar to the Mallier and Maslowe vortex array. Consequently, it is easy to show that the instability modes separate into two families, as in Refs. 11 and 14. Under the transformation of independent variables $(x,y)\to(x+L,-y)$, the symmetric mode transforms as $(u,v,w,\varpi)\to(u,-v,w,\varpi)$, while the antisymmetric mode transforms as $(u,v,w,\varpi)\to(-u,v,-w,-\varpi)$. In order to separate the symmetric and antisymmetric modes, we have to convert the representation of an arbitrary perturbation, given by Eq. (13) from exponential to trigonometric in y, while retaining the exponential dependence in x. This is merely an exercise in matrix manipulations. Once this is done we can identify the growth rates separately for the symmetric and

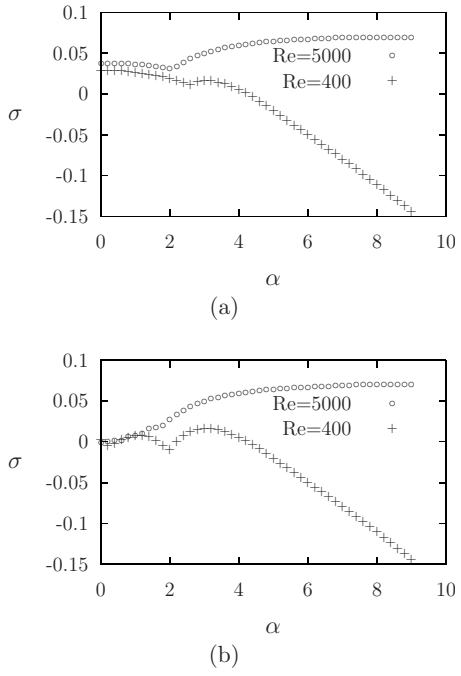

FIG. 1. Growth rate vs wavenumber for (a) symmetric and (b) antisymmetric modes for $r=1$, $k=k_1=0.3$ for Re=400 and 5000.

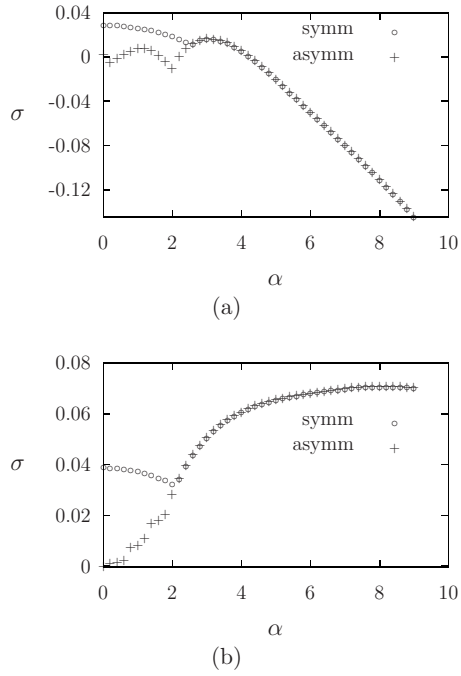

FIG. 2. Growth rate vs wavenumber for (a) Re=400 (b) Re=5000 for $r=1$, $k=k_1=0.3$ for both symmetric and antisymmetric modes.

antisymmetric modes. The doubly periodic array of vortices, given by Eq. (20) is periodic in y as well as in x and consequently symmetric and antisymmetric modes could also have been defined under transformation of independent variables $(x,y)\rightarrow(-x,y+L_1)$. Since the stream function ψ, given by Eq. (20), has similar dependence on x and y, we expect the results again would be similar to what we get considering symmetry under transformation of independent variables $(x,y)\rightarrow(x+L,-y)$.

III. RESULTS

We have computed growth rates σ, or more precisely the largest value of the real part of σ, for various values of the moduli, k and k_1, of the elliptic functions. We assume $r=1$, since altering the value of r would merely cause a uniform change in the size of the vortices without changing the shape or the velocity profiles. We first consider the situation where $k=k_1$. Then, by Eq. (22) we have $s=r$. Consequently $L=L_1$ and the vortex cells are square. The growth rates for the symmetric and antisymmetric modes for $k=k_1=0.3$ and Re =400 and 5000 are shown in Fig. 1. For Re=400 we have used $M=N=10$ in the representation given in Eq. (13), while for Re=5000 for which viscosity is less, we have used $M=N=12$.

We observe that, similar to the Mallier and Maslowe vortices, the symmetric mode has a nonzero growth rate even for two-dimensional perturbations, $\alpha=0$, while the growth rate for the antisymmetric mode vanishes as $\alpha\rightarrow 0$. For small viscosity, Re=5000, the highest growth rate, however, is obtained for nonzero values of α and appears to persist for larger values of α. For larger viscosity, Re=400, shorter wavelength perturbations are strongly damped. This short wavelength instability was explained in Ref. 14 to be due to the elliptical flow configuration. For small viscosity, Re =5000, the growth rate becomes almost independent of the wavenumber as expected of the elliptical instability. At this point, it would need some explanation why a short wavelength instability, which in Ref. 14 was explained to be due to the elliptical flow configuration[16–18] occurs even when the vortex cells are square, especially since in Ref. 19 it is argued that these are spurious modes. In Ref. 19, this instability was obtained but was removed by imposing certain symmetry conditions, which had been introduced earlier[30] by assuming the bounding box to be impenetrable. However, there seems no physical justification for assuming that the cell boundaries are impenetrable, there are no rigid walls at the cell boundaries. It appears that the initial result obtained in Ref. 19, that there is instability even when the vortex cells are square, is correct and there is physical reason to expect such instability. The so called elliptical instability would be expected to occur, even though the vortex cells are square, since the configuration is not azimuthally symmetric. So the rotating fluid would observe deviations from a purely circular azimuthally symmetric configuration and if this resonates with one of the natural frequencies of the system an instability can result. In Fig. 2, we plot the growth rate for the symmetric and antisymmetric modes together for comparison. We find that while the two are different for small values of α, beyond a certain value of α these become exactly identical. We now examine the complete spectrum. In Figs. 3 and 4, we show the spectrum for Re=400 and for $\alpha=1$ and $\alpha=3$. We observe that there are stationary, $\mathrm{Im}(\sigma)=0$, as well as traveling, $\mathrm{Im}(\sigma)\neq 0$, modes. While for $\alpha=1$, the most unstable mode is a traveling mode, for $\alpha=3$ the most unstable mode is a stationary mode. Even for $\alpha=3$ for symmetric modes there is also a traveling mode which is unstable, although the mode with the highest growth rate is stationary.

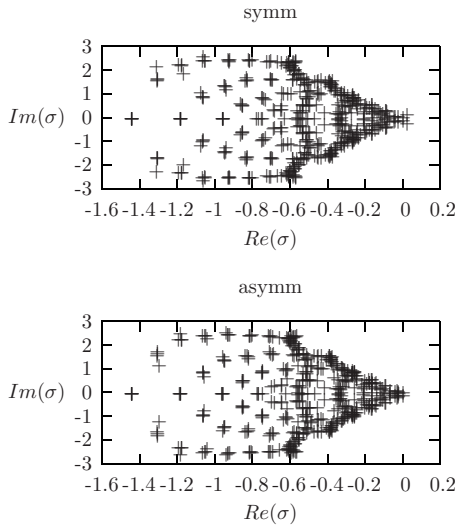

FIG. 3. The spectrum for $r=1$, $k=k_1=0.3$, Re=400, and $\alpha=1$ for symmetric and antisymmetric modes, shown in the complex σ plane.

We find that for Re=400 the most unstable mode is a traveling mode for long wavelengths but a stationary mode for short wavelengths. For Re=5000 the most unstable mode is always found to be a traveling mode. These observations are true for the symmetric as well as the antisymmetric modes. We have also computed the eigenfunctions. The contour plots of the perturbation in z-component of vorticity, given by $\partial v/\partial x - \partial u/\partial y$, together with quiver plots of the perturbation in velocity in the (x,y)-plane, for Re=400, for the most unstable antisymmetric mode for $\alpha=1$ and 3 are shown in Figs. 5 and 6. We study next the effect of changing the values of k and k_1 still assuming the two to be equal. The growth rates of the symmetric and antisymmetric modes for Re =400 and 5000 and for $k=k_1=0.4$ and 0.5 are shown in Figs. 7 and 8. For $k=k_1=0.5$, again examining the complete spectrum we find that the qualitative trends, when the most unstable mode is stationary and when it is a traveling mode, are

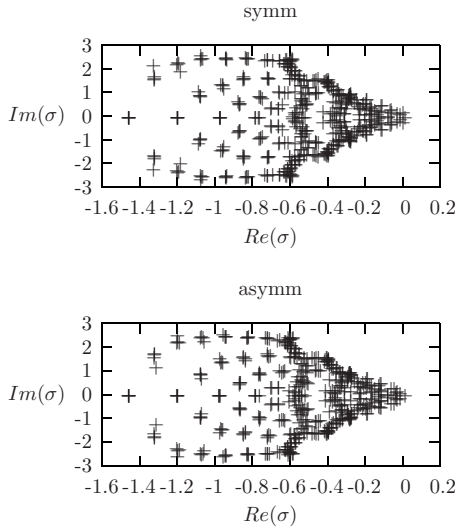

FIG. 4. The spectrum for $r=1$, $k=k_1=0.3$, Re=400, and $\alpha=3$ for symmetric and antisymmetric modes, shown in the complex σ plane.

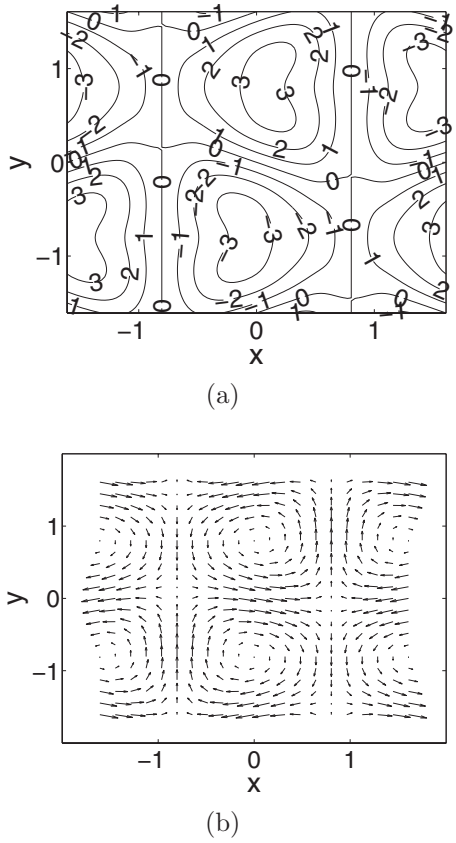

FIG. 5. Plots of (a) perturbation in the z-component of vorticity and (b) perturbation in the x- and y-components of velocity for the most unstable antisymmetric mode for $r=1$, $k=k_1=0.3$, Re=400, and $\alpha=1$.

similar to the trends for $k=k_1=0.3$. We observe that as the value of k and k_1 increase, the growth rates for small as well as large values of α become larger.

We now consider $k\neq k_1$. Consequently $r\neq s$ and the vortex cells are no longer square. The growth rates for $k=0.4$ and $k_1=0.2$ for Re=400 and 5000 are shown in Fig. 9. Now $L\approx 1.64$ and $L_1\approx 0.793\,79$ and there is significant ellipticity. Comparing with the results for $k=k_1$ we observe that the growth rates for $k=0.4$ and $k_1=0.2$ are higher than even for $k=k_1=0.4$, both for small as well as large values of α. Further we observe one more peak in the curves for growth rates. In Fig. 10, we plot the growth rates for the symmetric and antisymmetric modes together. Though for large wavenumbers the curves are similar, especially for small viscosity, the exact match between symmetric and antisymmetric modes that we observed for square vortex cells is no longer obtained. Again examining the complete spectrum for Re $=400,5000$ and $\alpha=0.5,2,4$ we find that the most unstable symmetric mode is a traveling mode except for Re=5000 and $\alpha=4$, while the most unstable antisymmetric mode is always a stationary mode.

IV. CONCLUSION

In this article we have studied the linear stability of one of the doubly periodic array of vortices given in Ref. 8. We have separated the instabilities into symmetric and antisymmetric modes. Comparing our results with Ref. 14, where the

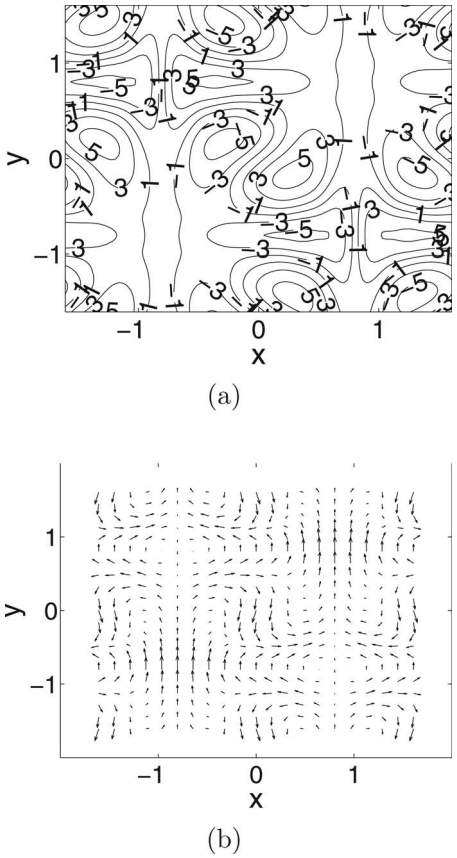

FIG. 6. Plots of (a) perturbation in the z-component of vorticity and (b) perturbation in the x- and y-components of velocity for the most unstable antisymmetric mode for $r=1$, $k=k_1=0.3$, Re=400, and $\alpha=3$.

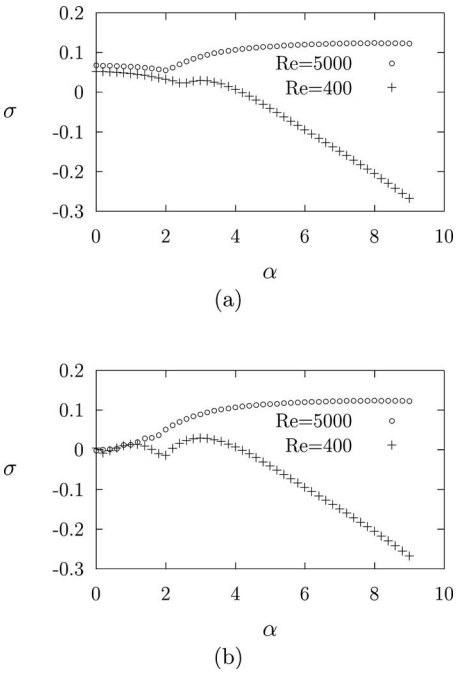

FIG. 7. Growth rate vs wavenumber for (a) symmetric and (b) antisymmetric modes for $r=1$, $k=k_1=0.4$ for Re=400 and 5000.

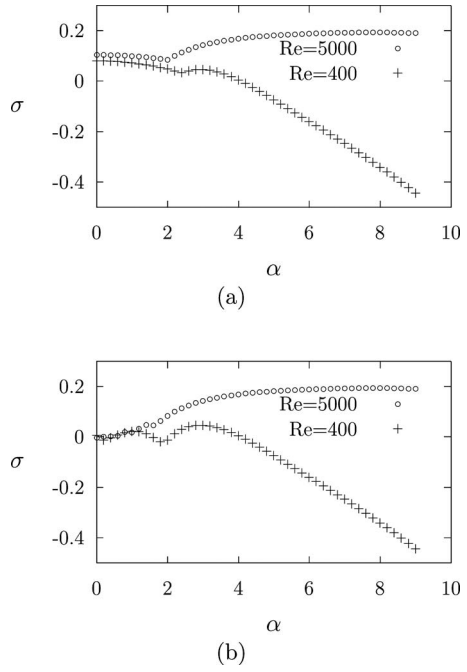

FIG. 8. Growth rate vs wavenumber for (a) symmetric and (b) antisymmetric modes for $r=1$, $k=k_1=0.5$ for Re=400 and 5000.

linear stability of the Mallier and Maslowe vortices was studied, we find that the qualitative trends are similar. For two-dimensional disturbances, $\alpha=0$, only the symmetric mode is unstable. For three-dimensional modes, for the antisymmetric mode we observe a peak in the growth rates at low values of α or large wavelength in the direction of the vortex axes. This was explained in Ref. 14 to be due to the Crow instability. For large values of α and for low values of viscosity

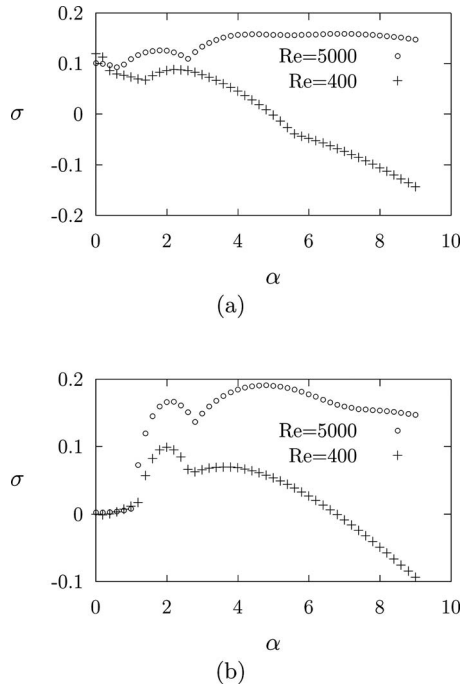

FIG. 9. Growth rate vs wavenumber for (a) symmetric and (b) antisymmetric modes for $r=1$, $k=0.4$ and $k_1=0.2$ for Re=400 and 5000.

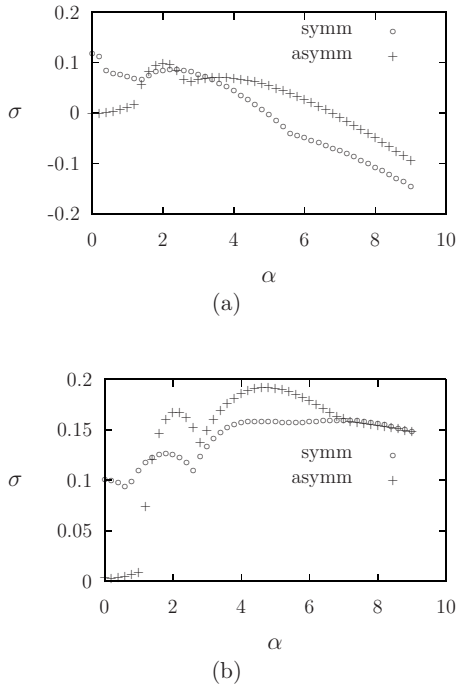

FIG. 10. Growth rate vs wavenumber for (a) Re=400 and (b) Re=5000 for $r=1$, $k=0.4$ and $k_1=0.2$ for both symmetric and antisymmetric modes.

we obtain growth rates which are almost independent of the wavenumber. For large values of α viscosity is found to stabilize the mode. Our study shows that the so called "elliptic instability" occurs even when the vortex cells are square. This was also found in Ref. 19 but was removed by imposing symmetry conditions which are appropriate if the cell boundaries are impermeable. We have argued that assuming the cell boundaries to be impermeable is not physically justified and, therefore, the instability for short wavelengths which is present even when the vortex cells are square is real and have given a physical reasoning why we would expect it to occur. However, as expected when the vortex cells are elongated the growth rates are higher. Further for square cells, beyond a certain wavenumber the growth rates of the symmetric and antisymmetric modes become exactly identical. This does not occur when the vortex cells are elongated. For elongated vortex cells we also observe more peaks in the graphs of growth rate versus wavenumber.

In this study we have considered the linear stability of one particular doubly periodic vortex array solution given in Ref. 8, and compared our findings with the earlier study of three-dimensional instabilities in a two-dimensional vortex array reported earlier in Ref. 19. We believe these bring out the essential trends. A stability study of other doubly periodic vortex array solutions given in Refs. 5–10 would certainly be relevant. A nonlinear stability study for three-dimensional perturbations would also be interesting. One limitation of the present analysis is that it does not consider subharmonic modes. Consequently the pairing instability is not modeled. These could form subjects for future studies.

[1]L. M. Milne-Thomson, *Theoretical Hydrodynamics* (Dover, New York, 1968).
[2]H. Lamb, *Hydrodynamics* (Cambridge University Press, Cambridge, England, 1932).
[3]J. T. Stuart, "On finite amplitude oscillations in laminar mixing layers," J. Fluid Mech. **29**, 417 (1967).
[4]R. Mallier and S. A. Maslowe, "A row of counter-rotating vortices," Phys. Fluids A **5**, 1074 (1993).
[5]K. W. Chow, N. W. M. Ko, and S. K. Tang, "Solitons in (2+0) dimensions and their applications in vortex dynamics," Fluid Dyn. Res. **21**, 101 (1997).
[6]K. W. Chow, N. W. M. Ko, R. C. K. Leung, and S. K. Tang, "Inviscid two dimensional vortex dynamics and a soliton expansion of the sinh-Poisson equation," Phys. Fluids **10**, 1111 (1998).
[7]B. N. Kuvshinov and T. J. Schep, "Double-periodic arrays of vortices," Phys. Fluids **12**, 3282 (2000).
[8]K. W. Chow, S. C. Tsang, and C. C. Mak, "Another exact solution for two-dimensional, inviscid sinh Poisson vortex arrays," Phys. Fluids **15**, 2437 (2003).
[9]D. Gurarie and K. W. Chow, "Vortex arrays for sinh-Poisson equation of two-dimensional fluids: Equilibria and stability," Phys. Fluids **16**, 3296 (2004).
[10]B. N. Kuvshinov and T. J. Schep, "Comment on 'Vortex arrays for sinh-Poisson equation of two-dimensional fluids: Equilibria and stability'," Phys. Fluids **17**, 079102 (2005).
[11]R. T. Pierrehumbert and S. E. Widnall, "The two- and three-dimensional instabilities of a spatially periodic shear layer," J. Fluid Mech. **114**, 59 (1982).
[12]T. Dauxois, "Nonlinear stability of counter-rotating vortices," Phys. Fluids **6**, 1625 (1994).
[13]T. Dauxois, S. Fauve, and L. Tuckerman, "Stability of periodic arrays of vortices," Phys. Fluids **8**, 487 (1996).
[14]S. Julien, J.-M. Chomaz, and J.-C. Lasheras, "Three-dimensional stability of periodic arrays of counter-rotating vortices," Phys. Fluids **14**, 732 (2002).
[15]S. C. Crow, "Stability theory for a pair of trailing vortices," AIAA J. **8**, 2172 (1970).
[16]R. T. Pierrehumbert, "Universal short-wave instability of two-dimensional eddies in an inviscid fluid," Phys. Rev. Lett. **57**, 2157 (1986).
[17]B. J. Bayly, "Three-dimensional instability of elliptical flow," Phys. Rev. Lett. **57**, 2160 (1986).
[18]F. Waleffe, "On the three-dimensional instability of strained vortices," Phys. Fluids A **2**, 76 (1990).
[19]D. Sipp and L. Jacquin, "Elliptic instability in two-dimensional flattened Taylor–Green vortices," Phys. Fluids **10**, 839 (1998).
[20]D. Montgomery and G. Joyce, "Statistical mechanics of 'negative temperature' states," Phys. Fluids **17**, 1139 (1974).
[21]D. Montgomery, W. H. Matthaeus, W. T. Stribling, D. Martinez, and S. Oughton, "Relaxation in two dimensions and the 'sinh-Poisson' equation," Phys. Fluids A **4**, 3 (1992).
[22]D. Montgomery, X. Shan, and W. H. Matthaeus, "Navier–Stokes relaxation to sinh-Poisson states at finite Reynolds numbers," Phys. Fluids A **5**, 2207 (1993).
[23]P. Tabeling, B. Perrin, and S. Fauve, "Instability of a linear array of forced vortices," Europhys. Lett. **3**, 459 (1987).
[24]P. Tabeling, S. Burkhart, O. Cardoso, and H. Willaime, "Experimental study of freely decaying two-dimensional turbulence," Phys. Rev. Lett. **67**, 3772 (1991).
[25]O. Cardoso, D. Marteau, and P. Tabeling, "Quantitative experimental study of the free decay of quasi-two-dimensional turbulence," Phys. Rev. E **49**, 454 (1994).
[26]N. N. Lebedev, *Special Functions and Their Applications* (Dover, New York, 1972).
[27]F. Bowman, *Introduction to Elliptic Functions with Applications* (Dover, New York, 1961).
[28]L. M. Milne-Thomson, *Jacobian Elliptic Function Tables* (Dover, New York, 1950).
[29]W. H. Press, S. A. Teukolsky, W. T. Vetterling, and B. P. Flannery, *Numerical Recipes in Fortran: The Art of Scientific Computing* (Cambridge University Press, Cambridge, England, 1992).
[30]T. S. Lundgren and N. N. Mansour, "Transition to turbulence in an elliptic vortex," J. Fluid Mech. **307**, 43 (1996).